processes

MDPI

Article

Diagenetic Evolution Control on Reservoir Quality of the Oligocene Weizhou Formation in Weixinan Sag of Beibuwan Basin, Northern South China Sea

Jinlai Huan [1], Yuanlin Meng [1], Qilin Wu [2,*], Lihua Xiao [1] and Zixuan Wang [2]

[1] School of Earth Sciences, Northeast Petroleum University, Daqing 163318, China; huanjl@cnooc.com.cn (J.H.); qhdmyl@163.com (Y.M.); 18249666848@163.com (L.X.)
[2] College of Petroleum Engineering, Guangdong University of Petrochemical Technology, Maoming 525000, China; 13580167684@163.com
* Correspondence: wuqilin666@126.com

Abstract: This study focuses on the diagenetic evolution of the reservoir in the third member of the Oligocene Weizhou Formation (E_3w_3) in Weinan Sag of Beibuwan Basin, northern South China Sea. Based on the contents and occurrence states of chlorite, illite, kaolinite and quartz cement were described by scanning electron microscopy (SEM), thin section and X-ray diffraction. In the E_3w_3 reservoir, three different occurrences of chlorite are recognized. These include chlorite coating, leaf-shaped chlorite and tongue-shaped chlorite. Furthermore, three major types of diagenetic kaolinite are observed. These include kaolin crystallization promoted by fluids of meteoric origin, kaolin formed by organic acids and blocky kaolin. In addition, feldspar, by organic acid dissolution, can mainly form kaolinite but also form illite or chlorite in the E_3w_3 reservoir. Different clay minerals have different effects on reservoir quality, which are controlled by occurrence and diagenetic environment. Compared to the other minerals, chlorite coating has a greater effect on quartz overgrowth. However, If minerals are packed in intergranular pores, they have a negative effect on reservoir quality.

Keywords: diagenesis; grain-coating chlorite; kaolinite; quartz overgrowth; beibuwan basin

Citation: Huan, J.; Meng, Y.; Wu, Q.; Xiao, L.; Wang, Z. Diagenetic Evolution Control on Reservoir Quality of the Oligocene Weizhou Formation in Weixinan Sag of Beibuwan Basin, Northern South China Sea. *Processes* **2023**, *11*, 2171. https://doi.org/10.3390/pr11072171

Academic Editors: Yinhui Zuo and Hui Han

Received: 18 June 2023
Revised: 11 July 2023
Accepted: 14 July 2023
Published: 20 July 2023

1. Introduction

Although sediment controls the inherent physical properties of the reservoir, diagenesis determines the ultimate reservoir quality. In the E_3w_3 reservoir, clay minerals, corrosion of feldspar and oil placement play an important role in the diagenetic process. They have a great effect on porosity and permeability, which are key properties of a petroleum reservoir [1]. For different clay minerals, it is important to study reservoir quality to understand the occurrence of clay minerals and the control factors on the occurrence of clay minerals [2]. There have been many studies on the effect of chlorite coats on reservoir quality [3–10]. In addition to chlorite coating, clay grain coats include illite coating [2,11], quartz overgrowth coating [12,13] and kaolinite coating [14]. Additionally, organic acids are also important to the dissolution of reservoirs, which result from the maturation of organic matter in shales or mudstone adjacent to sandstone [15]. In general, potassium feldspar is dissolved by organic acid to form kaolinite or illite [15–18]. However, K-feldspar may also be converted to chlorite from the analysis of the SEM in the E_3w_3 reservoir. Although at temperatures exceeding 70–80 °C, rates of authigenic quartz cementation become significant [19,20], quartz overgrowth was effectively inhibited by chlorite coating in the E_3w_3 reservoir. Previous researchers have conducted extensive research on reservoir quality in the study area [21–25], but there is little research on the control effect of diagenetic evolution on reservoir quality. From the analysis of XRD, SEM, thin section and core, it is more simple and feasible to determine the sequence of diagenetic evolution to observe the contact relation, symbiotic assemblage and dissolution filling characteristics of different authigenic minerals in the

reservoir [26,27]. Most importantly, we can understand the change in reservoir quality and its influencing factors, such as the occurrence of clay minerals, quartz overgrowth, oil placement and organic acid.

2. Geological Setting

Beibu bay basin is a tertiary sedimentary basin developed on the basis of prepaleogene bedrock, with an area of about 3.98 × 10^4 km^2. Weixinan Sag is located in the north of the Beibu bay basin, China. The study area is located in the Weixinan Sag and consists of three blocks: the North Block, Middle Block and South Block. The target layer is the third member of the Oligocene Weizhou Formation (E_3w_3), which was influenced by tectonic movements accompanied by the fault from activity to weakness (Figure 1a,b). Based on the core studies, the depositional environment of E_3w_3 has been interpreted to represent a delta front facies where the river enters the lake (Figure 1c). Affected by the sedimentary facies, the lithology is mainly sandstone, but there are mudstones of different thicknesses in the middle. This turbulent sedimentary feature leads to changes in the diagenetic environment, resulting in porosity and permeability varying greatly in the E_3w_3 reservoir.

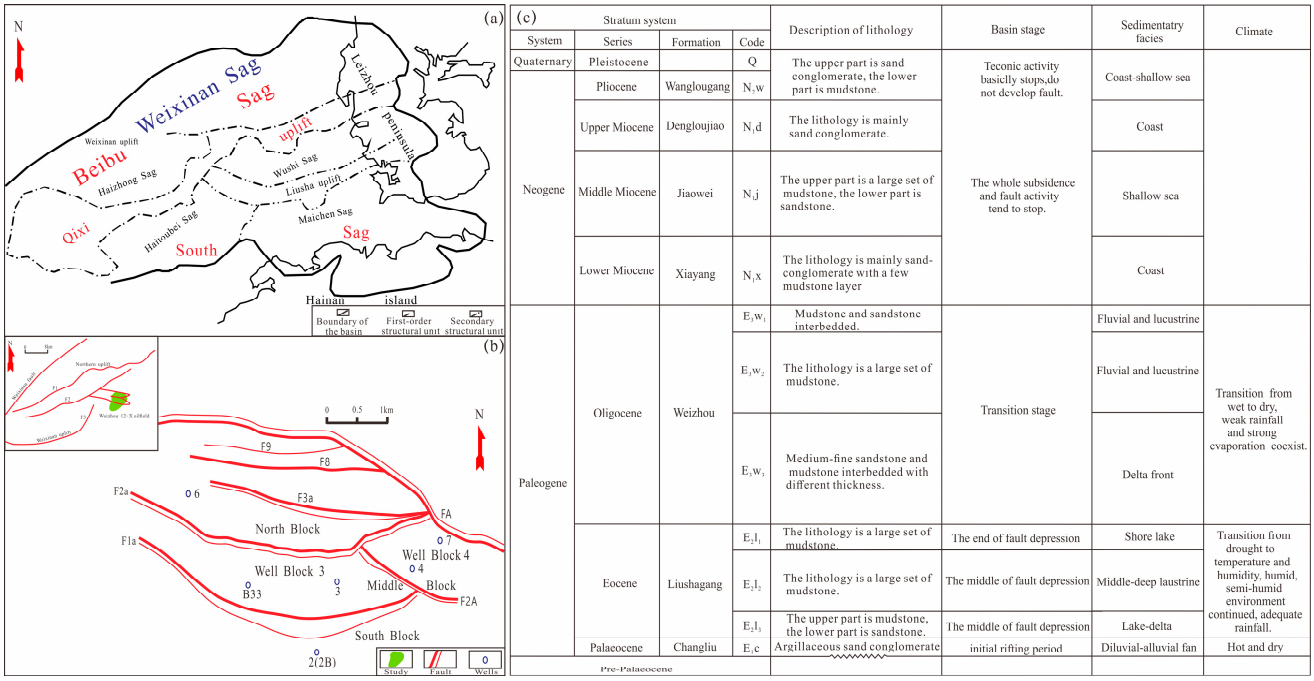

Figure 1. Division of tectonic units of Weixinan Sag (**a**), location of the study area (**b**) and stratigraphic characteristics of Weixinan Sag (**c**).

3. Petrographic and Micrological Analyses

3.1. Data Base

The database comprises 2446 samples, observed by microscopy of the thin sections (192 samples) and XRD analysis of bulk rock (180 samples). An SEM was also used (about 74 samples). All the samples were provided by CNOOC China Limited, Zhanjiang Branch, which also provided additional data such as grading analysis (438 samples) and whole rock analysis (30 samples).

3.2. Petrographic Description

The E_3w_3 Formation is a feldspathic quartz sandstone, fine to medium-grained, sandy sequence. There is a good correlation between particle size and mud content. The increase in grain size is accompanied by a reduction in shale content. The E_3w_3 Formation in well#3 has an average of 47.5–67.5% detrital quartz, including single-crystal and polycrystalline quartz (Figure 2). Quartz has a strong compressive resistance, which can hinder compaction,

and is beneficial to pore preservation [28]. It is relatively stable for the content of quartz overgrowth to vary between 0.5 and 2% (Figure 2). Quartz precipitation is influenced by temperature, pressure, PH and formation water properties. Feldspar content varies greatly, between 2 and 14%, which includes potassium feldspar and plagioclase. The E_3w_3 Formation has several carbonate cemented intervals, such as calcite, ferrocalcite, dolomite and ankerite (Figure 2). About 1.3% is usually present in the E_3w_3 Formation from well#3.

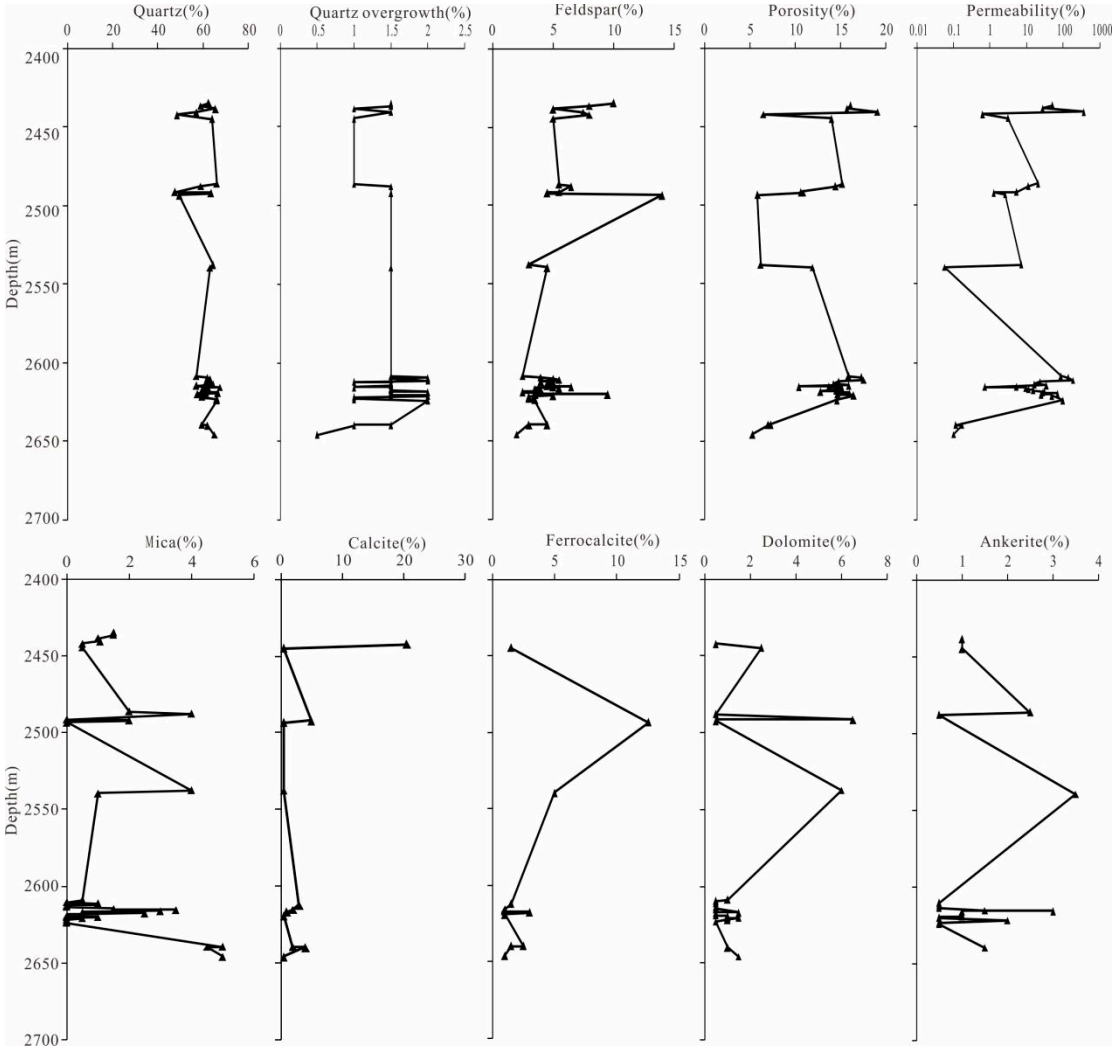

Figure 2. Results from analysis of microscopy of the thin sections. Well#3, E_3w_3 formation.

Core data for conventional porosity and permeability show high porosity at 2440 m and low porosity at 2493 m. The abnormal change in porosity is related to the irregular variation in cement content, especially calcite and ferrocalcite. Calcite (20.5%) or ferrocalcite (12.5%) cement has very low porosity.

3.3. Clay Minerals

Clay minerals are observed by SEM and analyzed by XRD. With the change in burial depth, the relative content of clay minerals is different. The relative content of chlorite (approximately 32%) is slightly higher than that of kaolinite (approximately 30%), followed by illite (approximately 24%) in well#3 (Figure 3). But chlorite began to transform into kaolinite at a depth of 2470 m to 2500 m in well#3 (Figure 3). The relative content of kaolinite (about 40%) was significantly higher than that of chlorite (approximately 22%) and illite (approximately 22%) in well#4 from the XRD data (Figure 3). Compared with well#4, the content of kaolinite (about 31%) is relatively low in well#7. The content of illite

and chlorite is still lower than kaolinite in well#7 (Figure 3). Kaolinite and illite have an obvious relationship between growth and decline from the XRD analysis data in well#7. At the same time, kaolinite and chlorite are positively correlated to a certain extent, which is different from well#3.

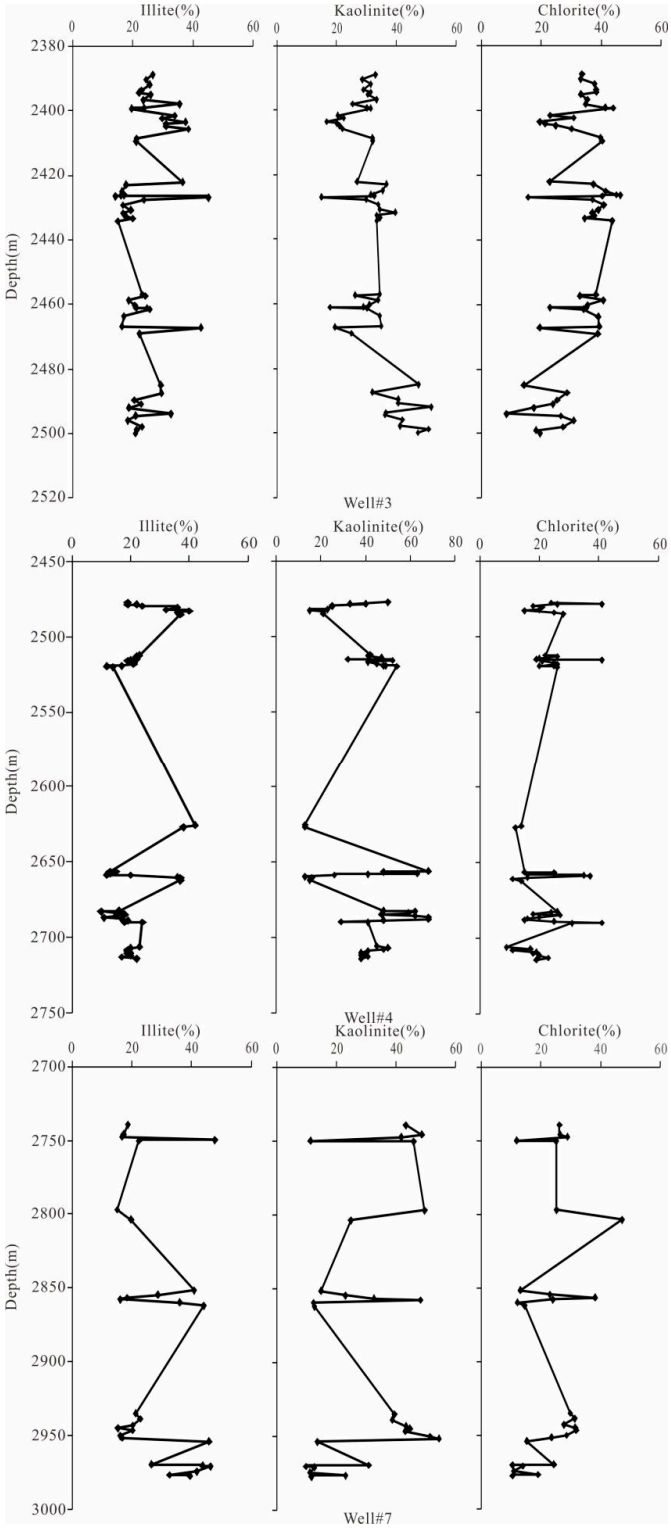

Figure 3. Results from the X-ray diffraction (XRD) analysis: Well#3; well#4; well#7.

4. Diagenetic Environment and Evolutionary Sequence

It is a more simple and feasible means for determining the sequence of diagenetic evolution to observe the contact relation, symbiotic assemblage and dissolution filling characteristics of different authigenic minerals in the reservoir [26,27]. The results from the microscopy of the thin section show that calcite and dolomite were formed in the early diagenetic stage (Figure 4a). And the formation time of ferric calcite and dolomite is later than that of calcite and dolomite (Figure 4b,c). Additionally, fine dolomite was replaced by ferrocalcite due to the addition of iron ions (Figure 4c). By scanning electron microscope, it was found that quartz cement is on the surface of the grain (Figure 5a,e). But the amount of quartz cement in the analyzed samples is clearly linked to the presence or absence of grain-coats anthigenic clays [11]. The amount of quartz cement in the E_3w_3 reservoir is controlled by chlorite attached to the surface of the particle. In addition, the precipitation time of quartz overgrowth is later than that of chlorite. The amount of quartz cement can be reduced if grain coats cover a large part of the surface of detrital quartz grains [8]. Therefore, chlorite coats can inhibit quartz cement and preserve porosity in the E_3w_3 reservoir. In the early diagenetic stage, there was acidic leaching of atmospheric water. Potassium feldspar was leashed and performed a honeycomb structure (Figure 5b). These phenomena indicate that the sequence of diagenetic evolution is calcite/dolomite → chlorite → quartz overgrowth → kaolinite. Therefore, the sequence of the diagenetic environment is acid → alkaline → acid. Additionally, there are corrosion pits on the surface of quartz secondary overgrowth (Figure 5c). The dissolution pit on the surface of the quartz particle is filled with kaolinite and chlorite (Figure 5h). In the middle diagenetic stage, kaolinite is mainly formed by organic acid entering the reservoir to dissolve feldspar and the transformation between clay minerals (Figures 3 and 5g). But, feldspar is dissolved to form not only kaolinite but also illite and chlorite (Figure 5d,i). Additionally, it was found that kaolinite cement was dissolved. These phenomena indicate that the sequence of the diagenetic environment is alkaline → acid → alkaline. Therefore, the diagenetic evolution of the E_3w_3 reservoir can be determined (Figure 6).

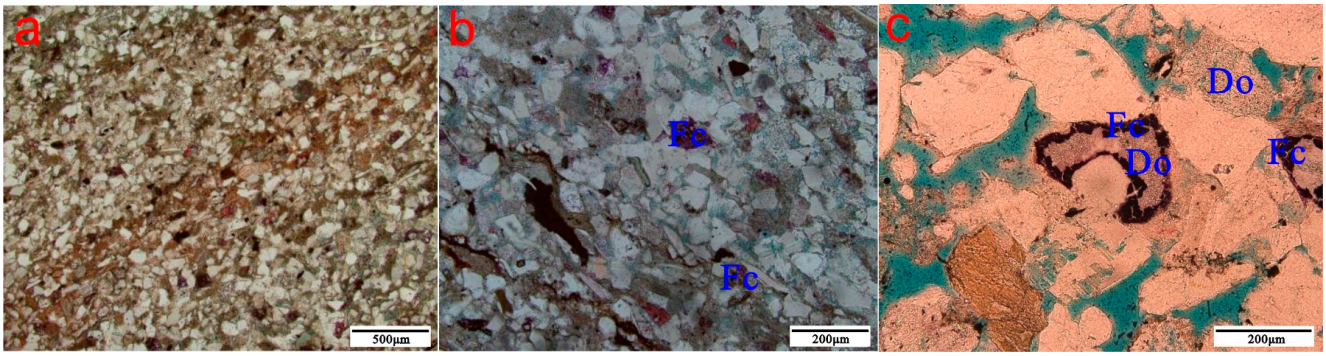

Figure 4. Analysis of microscopy of the thin sections: (**a**) Well#3,2448.47 m, (-) ×5, calcite cementation. (**b**) Well#3, 2447.24 m, (-) ×10, ferrocalcite cementation. (**c**) Well#4, 2516.17 m, (-) ×200, fine dolomite was replaced by ferrocalcite. Fc—ferrocalcite; Do—dolomite.

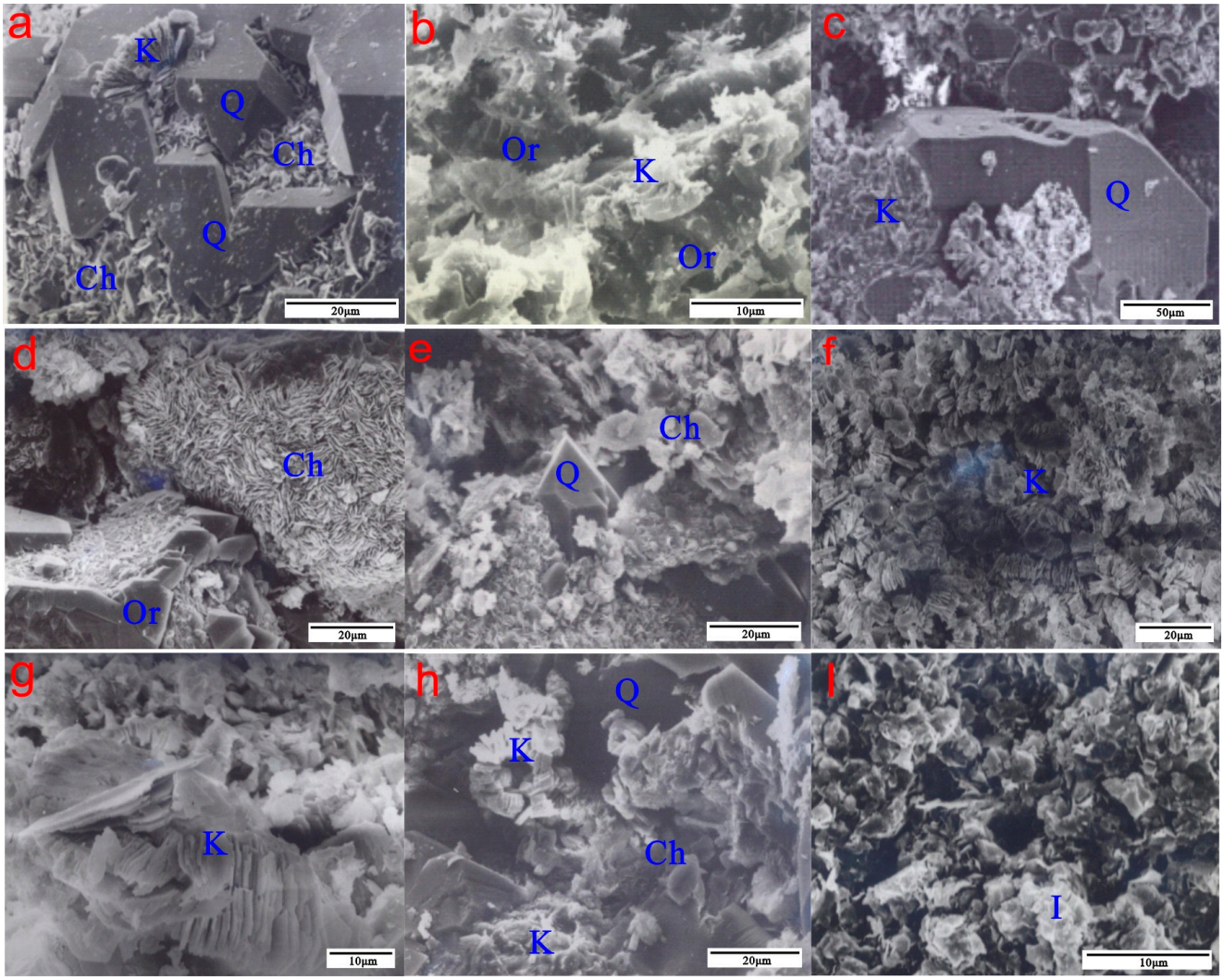

Figure 5. Analysis of scanning electron microscopy (SEM): (**a**) Well#2, 2360.92 m, ×1500; there are chlorite, quartz secondary overgrowth, kaolinite on the surface of grain. (**b**) Well#4, 2512.39 m, ×2940; potassium feldspar was leached by atmospheric water, and its shape is like a needle or rod. (**c**) Well#6, 2439.22 m, ×465; there are corrosion pits on the surface of quartz secondary overgrowth. (**d**) Well#2B, 2375.39 m, ×1260; feldspar transformed into chlorite, which is a leaf-shaped, filled between grains. (**e**) Well#4, 2713.37 m, ×1000; quartz secondary overgrowth III level formed later than the grain of chlorite. (**f**) Well#2B, 2375.39 m, ×815; kaolinite cement shrinkage and filled between grains. (**g**) Well#2B, 2393.05 m, ×1700; feldspar was dissolved and transformed into kaolinite. (**h**) Well#4, 2477.42 m, ×1180; kaolinite and chlorite were filled in the corrosion pit. (**i**) Well#2B, 2384.46 m, ×3400; feldspar was dissolved and transformed into illite. Ch—chlorite; Q—quartz; K—kaolinite; Or—potassium feldspar; I—illite.

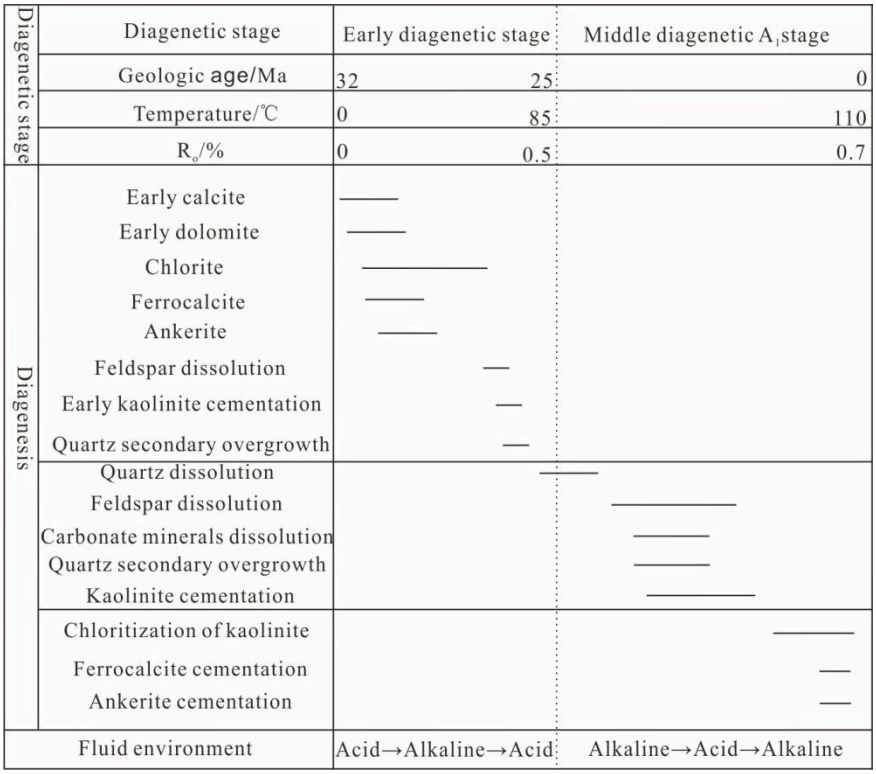

Figure 6. Diagenetic evolutionary sequence of E_3w_3 reservoir.

5. Discussion

5.1. Occurrence and Existing State

Chlorite is unstable under the physicochemical conditions of the Earth's surface but can form over a wide range of temperatures [29]. Most chlorite species existing in geological systems result from specific precursors except for direct precipitation due to dissolution. Furthermore, three main types of clay mineral series were reviewed by Beaufort et al. (2015): saponite-to-chlorite, berthierine-to-chlorite and kaolinite-to-sudoite reactions. In addition, the effect of chlorite coating in sandstones from different places is well known [3–10]. Micro-quartz [12,13], illite [2,11] and kaolinite [14] were also documented.

Many authors argued that the occurrence of chlorite is related to its genesis, but there is no one-to-one correspondence between the occurrence and genesis. In this paper, based on the results of previous studies, chlorite can be divided into four types: (1) chlorite coats are attached to the surface of the grain and wrap it [30–39]. It can inhibit a series of physical and chemical reactions of enveloped particles. In the E_3w_3 reservoir, the amount of quartz cement is reduced because chlorite coats cover the part of the detrital quartz. (2) Chlorite is attached to the surface of the pore throat [30,34–37,40–42]. It mainly affects the fluidity of pore fluid, especially permeability. (3) Chlorite is in the shape of a rose or leaf and is mainly filled in intergranular pores [22,23,30,34–37,39–41]. It occupies the pore space, which is unfavorable to the reservoir, and even plugs the throat. (4) Chlorite is globular or cellular [31,34]. In the E_3w_3 reservoir, the morphological characteristics of chlorite are mainly leaf-shaped (Figure 7a,e) and needle-shaped (Figure 7c), while tongue-shaped chlorite is rare (Figure 7d). The leaf-shaped aggregate of chlorite is globular or cellular; it can be only observed where feldspar is dissolved and transformed into chlorite (Figure 7a). Additionally, there are chlorites filling in the quartz secondary overgrowth (Figure 7f). From the analysis of SEM, the content of quartz cement is relatively low in the E_3w_3 reservoir; it is mainly affected by chlorite coats and oil emplacement. When chlorite coats cover the surface of quartz grains, it can restrain quartz overgrowth by preventing or reducing contact of quartz with fluid [3,42]. However, for chlorite in the filled pores, its effect on the quartz cement may not be as great or even insignificant; the effect of chlorite

on porosity and permeability cannot be ignored. Additionally, oil emplacement appears to have inhibited quartz cementation at high oil saturations and can be viewed as an important control of reservoir quality [43]. In the place with more oil, the content of quartz overgrowth is obviously less in the E_3w_3 reservoir. However, it is difficult to distinguish between chlorite and oil emplacement, which has a greater influence on quartz overgrowth.

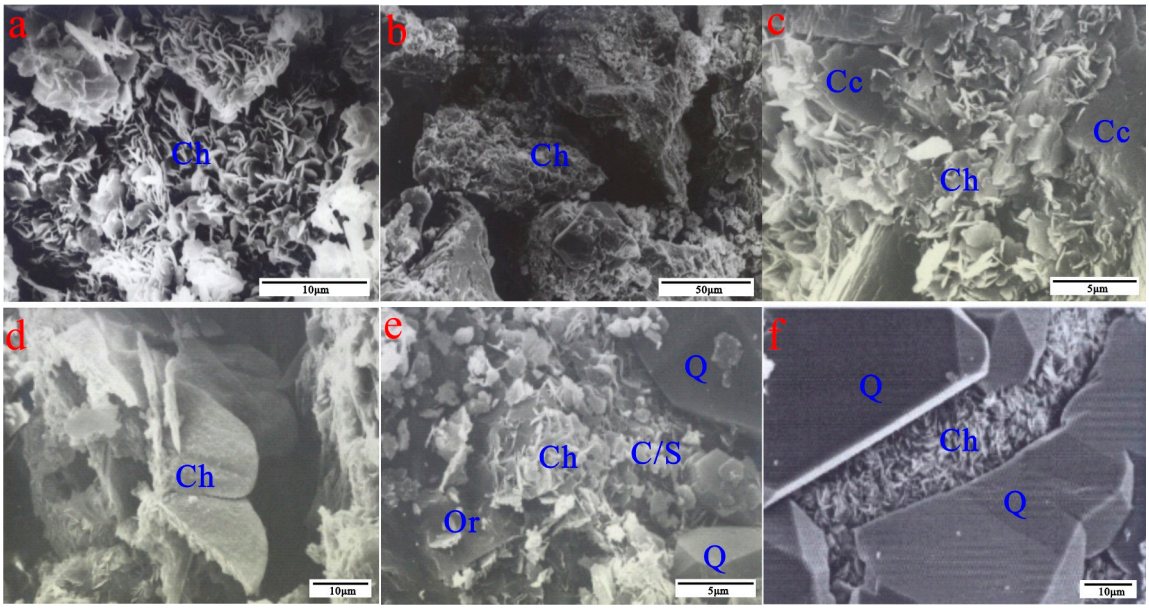

Figure 7. Results from scanning electron microscopy (SEM): (**a**) Well#2B, 2304.7 m, ×3100; feldspar was dissolved and transformed into chlorite. Chlorite is leaf-shaped. (**b**) Well#2B, 2355.7 m, ×510; there was chlorite coating. (**c**) Well#4, 2518.53 m, ×4570; chlorite was needle-shaped on the surface of grain. (**d**) Well#4, 2518.53 m, ×1630; chlorite was tongue-shaped. (**e**) Well#4, 2656.37 m, ×3870; there were C/S mixed layer and chlorite, which are filamentous and foliate, respectively. (**f**) Well#6, 2442.92 m, ×1510; there were chlorites filling in the quartz secondary overgrowth crystal. Ch—chlorite; Cc—calcite; Or—$KAlSi_3O_8$; C/S—C/S mixed layer; Q—quartz.

From the early Paleocene to the late Oligocene, the Beibuwan Basin experienced intense tension movement, and the large fault connected the deep magma heat source [44]. When the high-temperature magmatic-hydrothermal fluid moves to the shallow stratum and surface along the fault, the local geothermal field and fluid chemical properties near the migration channel would be affected, which was bound to affect the diagenesis of different types of rocks. When the high-temperature magmatic-hydrothermal solution carried a large amount of iron and magnesium plasma into E_3w_3, it promoted the transformation of smectite, kaolinite and feldspar to chlorite, resulting in the extreme development of chlorite in this period, and the common reaction formulas are as follows [45,46]:

$$2Ca_{0.1}Na_{0.2}Fe_{1.1}MgAlSi_{3.6}O_{10}(OH)_2 + 1.3Fe^{2+} + 1.5Mg^{2+} + 4Al^{3+} + 7.6H_2O = Fe_{3.5}Mg_{3.5}Al_6Si_6O_{20}\ OH)_{16} + 0.2Ca^{2+} + 0.4Na^{+} + 1.2SiO_2 + 16.8H^{+} \quad (1)$$

$$5CaMg(CO_3)_2 + Al_2Si_2O_5(OH)_4 + SiO_2 + H_2O = 5CaCO_3 + 5CO_2 + Mg_5Al_2Si_3O_{10}(OH)_8 \quad (2)$$

$$KAlSi_3O_8 + 1.4H_2O + 0.4Fe^{2+} + 0.3Mg^{2+} = 0.3(Fe_{1.4}Mg_{1.2}Al_{2.5})(Al_{0.7}Si_{3.3})O_{10}(OH)_8 + K^{+} + 0.4H^{+} + 2SiO_2 \quad (3)$$

Due to plenty of detailed investigations, most authors have shown the decisive influence of temperature on the occurrence of different kaolinite polytypes [47–50]. All these studies consistently show that morphological and structural modifications of kaolinite are continuous and related to temperature, depth or physicochemical properties of basin fluid [51–56].

In the E_3w_3 reservoir, three types of diagenetic kaolin are recognized: (1) kaolinnite is controlled by fluids of meteoric origin that flush the formation during early diagenesis (Figure 5b). However, it happens at a shallow depth [48,49,57]. (2) When organic acids entered the E_3w_3 reservoir, potassium feldspar was dissolved and converted to kaolinite (Figure 5g). (3) Dickite was recognized by scanning electron microscopy (SEM), which has a different occurrence compared with kaolinite. The model for the kaolinite-to-dickite transition: from the disordered kaolinite (Figure 8a) to ordered kaolinite (Figure 8b), then ordered dickite is present after the disordered. The diagenetic evolution of kaolin in sandstone was described in detail by Lanson et al. (2002).

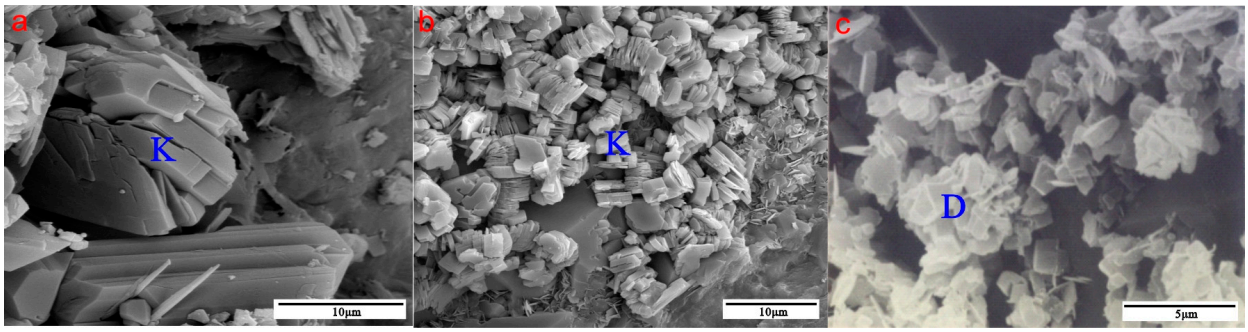

Figure 8. Occurrence of kaolinite observed by Scanning electron microscopy (SEM): (**a**) Well#B33, 2948.7 m, ×3500; pseudohexagonal flaky kaolinite. (**b**) Well#B33, 2197.4 m, ×2000; vermiform kaolinite. (**c**) Well#4, 2685.41 m, ×5450; dickite in the corrosion pit. K—kaolinite; D—dickite.

During the sedimentation period of the middle and late Weizhou Formation to Xiayang Formation, organic acids and CO_2 generated by the thermal evolution of organic matter entered E_3w_3 along the fault with the large-scale migration of oil and gas in the early stage, promoting the transformation of feldspar, illite and a small amount of chlorite to kaolinite, resulting in the extremely development of kaolinite. The common reaction formulas are as follows [58]:

$$2KAlSi_3O_8 + H_2O + 2H^+ \rightarrow Al_2Si_2O_5(OH)_4 + 4SiO_2 + 2K^+ \quad (4)$$

$$K_{0.6}Mg_{0.25}Al_{2.3}Si_{3.5}O_{10}(OH)_2 + 1.1H^+ \rightarrow 1.15Al_2Si_2O_5(OH)_4 + 1.2SiO_2 + 0.6K^+ + 0.25Mg^{2+} \quad (5)$$

$$Fe_{3.5}Mg_{3.5}Al_6Si_6O_{20}(OH)_{16} + 14H^+ \rightarrow 3.5Fe^{2+} + 3.5Mg^{2+} + 9H_2O + Al_2Si_2O_5(OH)_4 \quad (6)$$

The above multiple reactions can occur at different times or simultaneously, but the difficulty of their reactions varies significantly depending on the geological conditions of different basins. This can be studied through the calculation results of Gibb's free energy increment in thermodynamics [59]. When the free energy increment $\Delta G > 0$, the process cannot occur automatically; when $\Delta G < 0$, the process automatically occurs. In this paper, the free energy increment of transformation from kaolinite to illite, kaolinite to chlorite (Equation (2)), illite to kaolinite (Equation (5)), and chlorite to kaolinite (Equation (6)) was calculated, respectively, through temperature and pressure data (Figure 9). The results show that the free energy increment of the transformation from kaolinite to illite is positive, indicating that the reaction cannot occur automatically. The free energy increments of the other three reactions (Equations (2), (5) and (6)) are all negative, indicating that the three reactions can occur automatically underground. In addition, numerically, the free energy increment from kaolinite to chlorite is far less than that from kaolinite to illite (Figure 9); the free energy increment from illite to kaolinite is less than that from chlorite to kaolinite (Figure 9). That is, under alkaline conditions, the transformation from kaolinite to chlorite is much easier than that from kaolinite to illite. Under acidic conditions, the conversion of illite to kaolinite is easier than that of chlorite to kaolinite.

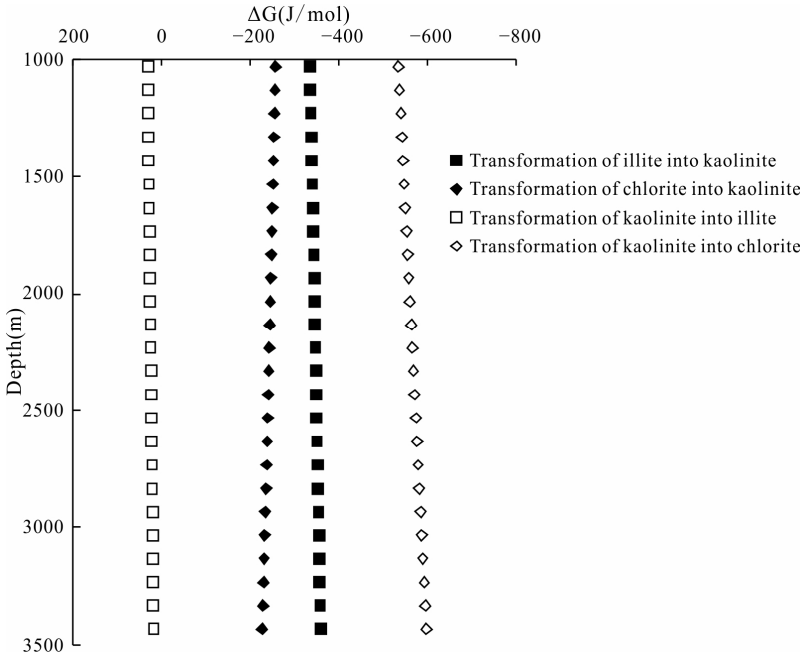

Figure 9. Free energy increment of clay mineral transformation in Weixinan Sag.

5.2. Dissolution of Feldspar

It is well known that potassium feldspar is dissolved to form kaolinite [60]. But it is comparatively rare that feldspar is dissolved to form illite or chlorite, especially chlorite. The replacement of K-feldspar by kaolinite or illite is sensitive to the PH and the activity of aqueous potassium. However, iron and magnesium ions are the basis of the formation of chlorite [34,61,62]. Currently, more recognized sources of iron and magnesium are as follows: (1) Rivers can carry iron and magnesium ions [3]. (2) Volcanic debris is hydrolyzed. (3) The mudstone is compacted and dehydrated [63]. (4) External fluids carry iron and magnesium ions [32].

In the E_3w_3 reservoir, feldspar is dissolved mainly to form kaolinite from the analysis of XRD and SEM. But, K-feldspar can also be replaced by illite or chlorite (Figure 5d,i and Figure 7a). Transformation of K-feldspar to kaolinite or illite can be expressed by the following equations, respectively:

$$2KAlSi_3O_8 + H_2O + 2H^+ = Al_2Si_2O_5(OH)_4 + 4SiO_2 + 2K^+ \quad (7)$$

$$3KAlSi_3O_8 + 2H^+ = KAl_3Si_3O_{10}(OH)_2 + 6SiO_2 + 2K^+ \quad (8)$$

Equations (7) and (8) show that the transformation of K-feldspar to kaolinite and illite occurred in an acidic diagenetic environment. However, chlorite is formed in an alkaline diagenetic environment. In the early diagenetic stage, the strong hydrolysis of igneous rock debris in sandstone and the large amount of iron and magnesium ions carried by rivers provide favorable conditions for the formation of chlorite. Additionally, C/S mixed layer is observed by SEM (Figure 7e). It indicates that there is a transformation of smectite to chlorite [64]:

$$\begin{aligned} Ca_{0.1}Na_{0.2}Fe_{1.1}MgAlSi_{3.6}O_{10}(OH)_2 + 1.5Fe^{2+} + 1.2Mg^{2+} + 1.4Al^{3+} + 7.6H_2O = \\ = Fe_{3.5}Mg_{3.5}Al_6Si_6O_{20}(OH)_{10} + 0.1Ca^{2+} + 0.2Na^+ + 0.8SiO_2 + 9.2H^+ \end{aligned} \quad (9)$$

Although feldspar to chlorite conversion is relatively rare, during the transformation of smectite into illite, the content of chlorite in mudstone increased obviously [65]:

$$\text{K-feldspar} + \text{smectite} \rightarrow \text{illite} + \text{chlorite} + \text{quartz} \quad (10)$$

The dissolution of micrograined feldspar in low-temperature alkaline solution was studied [66], and the results show that the solubility of micrograined feldspar increases with the increase in pH. This result also coincides with the previous research results [67]. Therefore, feldspar transforms into chlorite in an alkaline environment. There may be the following equation:

$$2KAlSi_3O_8 + 14H_2O + 3.5Fe^{2+} + 3.5Mg^{2+} = Fe_{3.5}Mg_{3.5}Al_6Si_6O_{20}(OH)_{10} + K^+ + 18H^+ \quad (11)$$

In the E_3w_3 reservoir, kaolinite and chlorite are a positive correlation in the transition zone between sandstone and mudstone (Figure 10). However, kaolinite in sandstone is a negative correlation with chlorite (Figure 10). This has been mainly attributed to higher porosity and permeability in sandstone compared to mudstone [68,69]. Therefore, we need to understand the effects of an open system vs. a closed system on changes in clay mineralogy [69]. The mutual reaction between kaolinite and chlorite can happen in an open system, while the reaction may be inhibited by a closed system because the products of the reaction cannot be carried out by the fluid due to lower porosity and permeability. At the same time, the transformation of potash feldspar to chlorite also tends to react in closed systems.

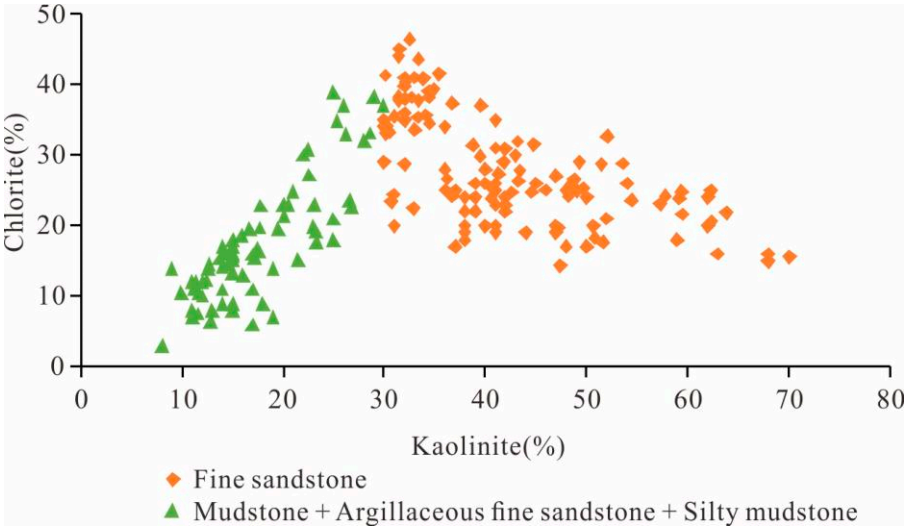

Figure 10. Relationship between chlorite and kaolinite from the analysis of XRD.

5.3. Reservoir Quality

In the E_3w_3 reservoir, kaolinite always has a positive effect on porosity (Figure 11a). In general, the reservoir with a higher content of kaolinite is often accompanied by stronger dissolution and more secondary porosity, which is beneficial to improve reservoir quality, but illite always has a negative effect on porosity (Figure 11b), and the effect of the I/S mixed layer on reservoir porosity is similar to that of illite (Figure 11f). However, the influence of chlorite on reservoir quality is complicated and is different from well to well. Chlorite has a negative effect on the porosity in well#4 (Figure 11e), while chlorite has a positive effect on the porosity in well#3 (Figure 11c). In addition, chlorite has both positive and negative effects on porosity in well#7 (Figure 11d). The result may be related to the number of samples. Mostly, it is difficult to determine the morphological characteristics and occurrence state of each chlorite sample in the reservoir.

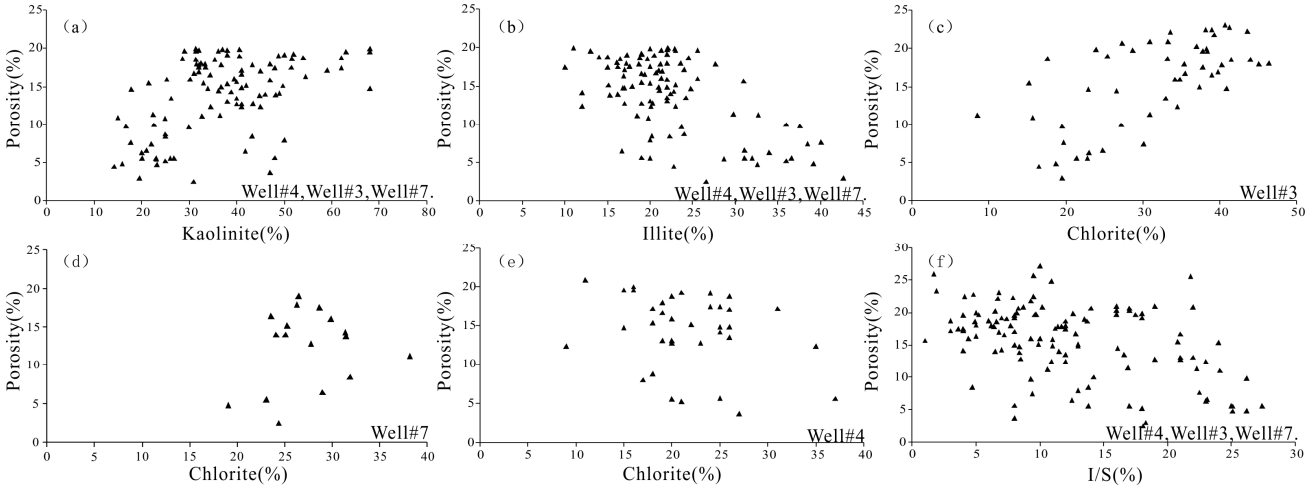

Figure 11. The effect of clay minerals on porosity in the E_3w_3 reservoir: (**a**) Kaolinite has a positive effect on porosity. (**b**) Illite has a negative effect on porosity. (**c**) Chlorite has a positive effect on the porosity in well#3. (**d**) Chlorite has both positive and negative effects on the porosity in well#7. (**e**) Chlorite has a negative effect on the porosity in well#4. (**f**) The I/S mixed layer has a negative effect on porosity.

XRD diffraction, laser particle size, and physical property analysis data indicate that the types and contents of authigenic clay minerals with different particle sizes have different control effects on reservoir permeability (Figure 12). Taking the typical well#4 as an example, when the clastic particles are medium sandstone, the reservoir permeability is high. In terms of numerical value, when the content of kaolinite, illite, I/S mixed layer and chlorite is high or low, the change in reservoir permeability is relatively small, and the difference between the maximum and minimum values is about 1~2 orders of magnitude. When the clastic particles are, respectively, fine sandstone and extremely fine sandstone, the content of kaolinite, illite, I/S mixed layer and chlorite has a significant control on the permeability, and the maximum and minimum permeability of the reservoir differ by about three and four orders of magnitude, respectively. Among them, the content of kaolinite and chlorite is positively correlated with the overall permeability. The main reason is that the genesis of kaolinite and chlorite is related to the deep magmatic-hydrothermal solution, organic acid and CO_2, which is more constructive than the precipitation effect of authigenic clay itself [22], increasing the porosity and permeability of the reservoir. The illite and I/S mixed layer have a negative correlation with permeability. The main reason is that the illite and I/S mixed layer often bridges the pore throat or fills the intergranular pores, reducing the reservoir porosity and permeability. Therefore, the particle size of detrital particles significantly restricts the influence of clay minerals on reservoir physical properties. The finer the particle size of detrital particles is, the weaker the control effect of particle size on permeability, the stronger the influence of clay minerals on permeability, and the greater the order of magnitude difference between the maximum and minimum values of permeability.

There are three abnormally high porosity and permeability zones (I~III zone) vertically developed in the reservoir of the study area (Figure 13), with depths ranging from 2300 m to 2400 m, 2400 m to 2600 m, and 2600 m to 2900 m [21]. There are significant differences in the diagenetic stages, diagenetic facies, clay mineral content, and types of different abnormal high porosity and permeability zones.

The I zone is in the middle A_1^1 stage of diagenesis, with early weak dissolution facies developed. The content of chlorite is low, ranging from 12 to 35.7%, with an average of 23.6%. The content of kaolinite is relatively high, ranging from 11 to 70.1%, with an average of 44.5%. The content of illite is low, ranging from 11 to 60.1%, with an average of 22.8%.

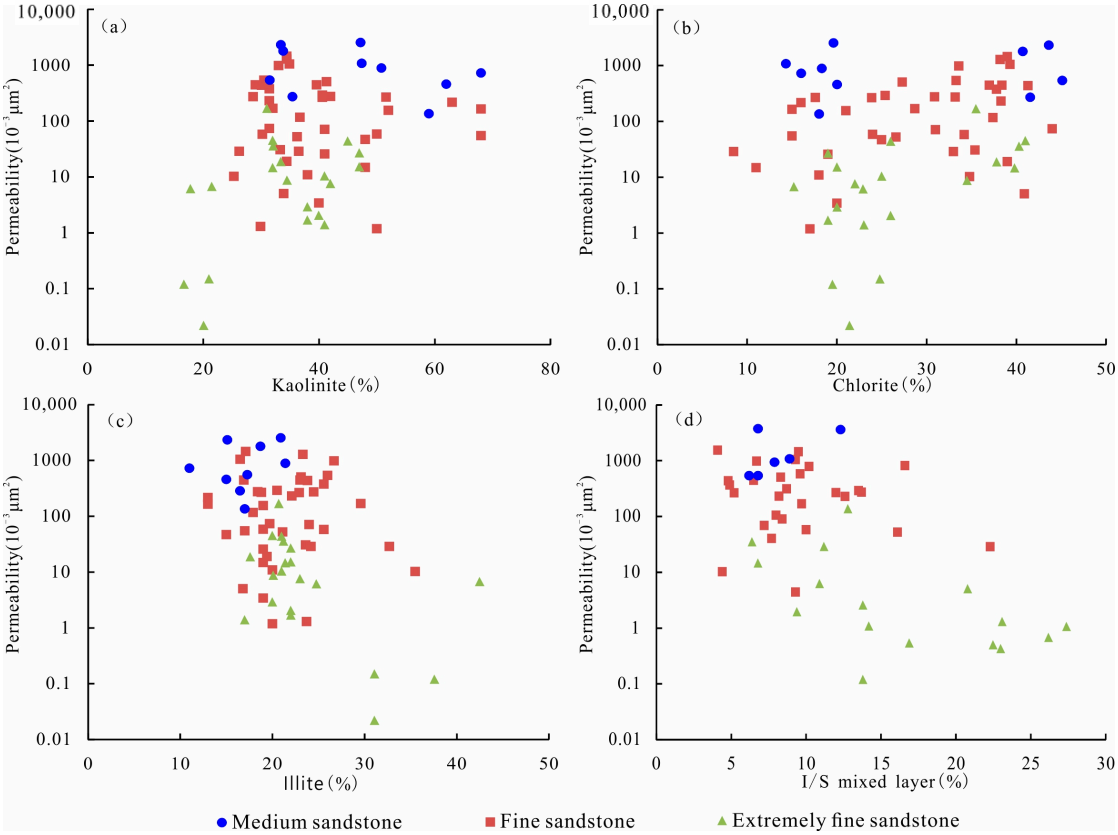

Figure 12. The effect of clay minerals on permeability under different particle sizes in the E_3w_3 reservoir: (**a**) Kaolinite has a positive effect on permeability as a whole. (**b**) Chlorite has a positive effect on permeability as a whole. (**c**) Illite has a negative effect on permeability. (**d**) The I/S mixed layer has a negative effect on permeability.

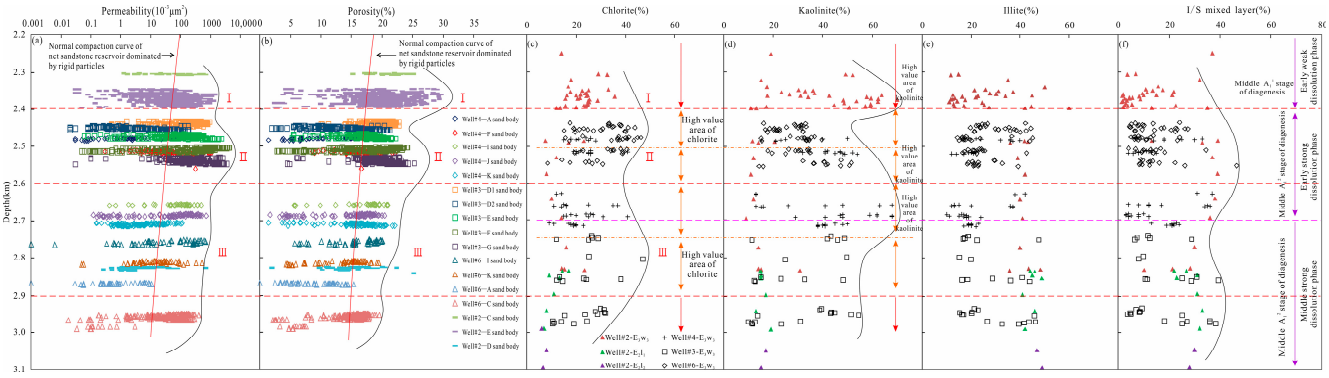

Figure 13. Differential control effect of diagenesis on different abnormal high porosity and permeability zones: (**a**) Vertical distribution of abnormal high permeability zones. (**b**) Vertical distribution of abnormal high porosity zones. (**c**) Evolution trend of relative content of chlorite with burial depth. (**d**) Evolution trend of relative content of kaolinite with burial depth. (**e**) Evolution trend of relative content of illite with burial depth. (**f**) Evolution trend of relative content of I/S mixed layer with burial depth.

The II zone is in the middle A_1^2 stage of diagenesis, with early development of strong dissolution facies. The upper part of it has been eroded by alkaline hydrothermal fluid, with a depth of 2400~2500 m. The content of chlorite is high, between 15 and 46.4%, with an average of 30.9%. The content of kaolinite and illite is similar, ranging from 15 to 50% and 14.3 to 45.2%, with an average of 27.8% and 27.7%. The lower part of it has experienced the

erosion of organic matter acidic thermal fluid, with a depth of 2500 m~2600 m. The content of kaolinite is high, between 11 and 59%, with an average value of 36.3%. The content of chlorite is lower, between 8 and 41%, with an average of 25.5%. The content of illite is the lowest, ranging from 12 to 42.7%, with an average of 23.6%.

The III zone is in the middle A_1^2 stage of diagenesis, with strong dissolution facies in the middle development stage. The content of kaolinite is the highest, between 9 and 68%, with an average of 34.5%. The content of illite is lower, ranging from 10 to 48.9%, with an average of 27.5%. The content of chlorite is the lowest, ranging from 9 to 41%, with an average of 18.8%.

In summary, the formation of abnormal high porosity and permeability zones in the Weixinan Sag is closely related to the abnormal transformation of clay minerals. The formation of the I zone is mainly related to kaolinization, the formation of the III zone is mainly related to chloritization, and the formation of the II zone is the result of the joint action of kaolinization and chloritization.

6. Conclusions

It is important to determine the diagenetic evolution of the E_3w_3 reservoir because it can give us much geological information. In the early diagenetic stage, early calcite and dolomite start to precipitate. Calcite and dolomite were replaced by ferrocalcite and ankerite when the diagenetic environment changed from acidic to alkaline.

At the same time, chlorite began to form because there was enough iron and magnesium. In the middle diagenetic stage, as organic acids enter the reservoir, feldspar is dissolved, which is mainly converted into kaolinite, but also into illite or chlorite. Different clay minerals have different effects on reservoir quality. In general, kaolinite always has a positive effect on the reservoir quality, and illite always has a negative effect on the reservoir quality. However, the effect of chlorite on reservoir quality is influenced by occurrence, existing state, and diagenetic environment.

Different clay minerals have different controls on reservoir physical properties. Kaolinization has an important influence on the formation of the first abnormal high porosity and permeability zone, and chloritization has an important control on the formation of the third abnormal high porosity and permeability zone. The formation of the second abnormal high porosity and permeability zone is the result of the combination of kaolinization and chloritization.

Author Contributions: Conceptualization, J.H. and Q.W.; methodology, Y.M.; investigation, Z.W.; writing—original draft preparation, J.H., Y.M., Q.W. and L.X.; writing—review and editing, J.H., Z.W. and Q.W. All authors have read and agreed to the published version of the manuscript.

Funding: This research was funded by Major Projects of National Science and Technology (Grant No. 2016ZX05046-001-006), the National Natural Science Foundation of China (Grant No. 41572135), and the Innovation Project of Educational Commission of Guangdong Province of China (Grant 2020KTSCX084).

Data Availability Statement: Our research data is authentic and reliable, but the data is unavailable due to privacy or ethical restrictions. If any scholars are interested in the process, they can contact the authors to obtain.

Acknowledgments: We thank the China National Offshore Oil Company for permission to release the data.

Conflicts of Interest: The authors declare no conflict of interest.

References

1. Freiburg, J.T.; Ritzi, R.W.; Kehoe, K.S. Depositional and diagenetic controls on anomalously high porosity within a deeply buried CO_2 storage reservoir—The Cambrian Mt.Simon Sandstone, Illinois Basin, USA. *Int. J. Greenh. Gas Control* **2016**, *55*, 42–45. [CrossRef]
2. Hansen, H.N.; Løvstad, K.; Müller, R.; Jahren, J. Clay coats preserving high porosities in deeply buried intervals of the Stø Formation. *Mar. Pet. Geol.* **2017**, *88*, 648–658. [CrossRef]

3. Ehrenberg, S.N. Kaolinized, potassium-leached zones at the contacts of the Garn Formation, Haltenbanken, mid-Norwegian continental shelf. *Mar. Pet. Geol.* **1991**, *8*, 250–269. [CrossRef]
4. Ehrenberg, S.N.; Dalland, A.; Nadeau, P.H.; Mearns, E.W.; Amundsen, H.E.F. Origin of chlorite enrichment and neodymium isotopic anomalies in Haltenbanken sandstones. *Mar. Pet. Geol.* **1998**, *15*, 403–425. [CrossRef]
5. Jahren, J.; Olsen, E.; Bjørlykke, K. Chlorite coatss in deeply buried sandstones—Examples from the Norwegian shelf. In *Water–Rock Interaction*; Arehart, G.B., Hulston, J.R., Eds.; Balkema: Rotterdam, The Netherlands, 1998; pp. 321–324. ISBN 905410942.
6. Olsen, E. Et Diagenetisk Studie av Dypt Begravde Sandsteiner fra Haltenbanken, Med Spesiell Vekt på Klorittbelegg. Unpublished Cand. Scient. Ph.D. Thesis, University of Oslo, Oslo, Norway, 1996; p. 161.
7. Dixon, S.A.; Summers, D.M.; Surdam, R.C. Diagenesis and preservation of porosity in Norphlet Formation (Upper Jurassic), Southern Alabama. *Am. Assoc. Pet. Geol. Bull.* **1989**, *73*, 707–728.
8. Heald, M.T.; Larese, R.E. Influence of coatss on quartz cementation. *J. Sediment. Petrol.* **1974**, *44*, 1269–1274.
9. Pittman, E.D.; Larese, R.E.; Heald, M.T. *Clay Coats: Occurrence and Relevance to Preservation of Porosity in Sandstones*; Houseknecht, D.W., Pittman, E.D., Eds.; Society of Economic Paleontologists and Mineralogists (Special Publication): Tulsa, OK, USA, 1992; Volume 47, pp. 241–255.
10. Ryan, P.C.; Reynolds, R.C., Jr. The origin and diagenesis of grain coats serpentine-chlorites in Tuscaloosa Formation Sandstone, U.S. Gulf Coast. *Am. Mineral.* **1996**, *81*, 213–225. [CrossRef]
11. Storvoll, V.; Bjørlykke, K.; Karlsen, D.; Saigal, G. Porosity preservation in reservoir sandstones due to grain-coats illite: A study of the Jurassic Garn Formation from the Kristin and Lavrans fields, offshore Mid-Norway. *Mar. Petrol. Geol.* **2002**, *19*, 767–781. [CrossRef]
12. Ramm, M.; Forsberg, A.W.; Jahren, J.S. Porosity–depth trends in deeply buried Upper Jurassic reservoirs in the Norwegian Central Graben: An example of porosity preservation beneath the normal economic basement by grain-coats microquartz. In *Reservoir Quality Prediction in Sandstones and Carbonates*; Kupecz, J.A., Gluyas, J., Bloch, S., Eds.; American Association of Petroleum Geologists Memoir: Tulsa, OK, USA, 1997; Volume 69, pp. 61–77.
13. Spark, I.S.C.; Trewin, N.H. Facies-related diagenesis in the main claymore oilfield sandstones. *Clay Miner.* **1985**, *21*, 479–496. [CrossRef]
14. Walderhaug, O.; Bjørkum, P.A.; Aase, A.E. Kaolin-coats of stylolites, effect on quartz cementation and general implications for dissolution at mineral interfaces. *J. Sediment. Res.* **2006**, *76*, 234–243. [CrossRef]
15. Lanson, B.; Beaufort, D.; Berger, G. Authigenic kaolin and illitic minerals during burial diagenesis of sandstones: A review. *Clay Miner.* **2002**, *37*, 1–22. [CrossRef]
16. Gaupp, R.; Matter, A.; Platt, J.; Ramseyer, K.; Walzebuck, J. Diagenesis and fluid evolution of deeply buried Permian (Rotliegende) gas reservoir, Northwest Germany. *Am. Assoc. Pet. Geol. Bull.* **1993**, *77*, 1111–1128.
17. Platt, J.D. Controls on clay mineral distribution and chemistry in the early Permian Rotliegend of Germany. *Clay Miner.* **1993**, *28*, 393–416. [CrossRef]
18. Berger, G.; Lacharpagne, J.-C.; Velde, B.; Beaufort, D.; Lanson, B. Kinetic constraints for mineral reactions in sandstone/shales sequences and modelling of the effect of the organic diagenesis. *Appl. Geochem.* **1997**, *12*, 23–35. [CrossRef]
19. Mcbride, E.F. Quartz cement in sandstones: A review. *Earth-Sci. Rev.* **1989**, *26*, 69–112. [CrossRef]
20. Bjørlykke, K.; Egeberg, P.K. Quartz cementation in sedimentary basins. *AAPG Bull.* **1993**, *77*, 1538–1548.
21. Chen, G.S.; Meng, Y.L.; Huan, J.L.; Wang, Y.C.; Zhang, L.; Xiao, L.H. Distribution and origin of anomalously high permeability zones in Weizhou Formation, Weizhou 12-X oilfield, Weixinan Sag, China. *Earth Sci. Inform.* **2021**, *1*, 1–13. [CrossRef]
22. Chen, G.S.; Meng, Y.L.; Huan, J.L.; Dai, T.J.; Xiao, L.H.; Zhou, W. Quantitative evaluation of impact of authigenic chlorite on reservoir quality: A case study of the Member 3 of Weizhou Formation in Weixinan sag, Beibu Gulf Basin. *J. Palaeogeogr.* **2021**, *23*, 640–650. (In Chinese)
23. Zheng, Z.Y.; Zuo, Y.H.; Wen, H.G.; Zhang, J.Z.; Zhou, G.; Xu, L.; Sun, H.F.; Yang, M.H.; Yang, K.N.; Zeng, J.C. Natural gas characteristics and gas-source comparisons of the Lower Triassic Jialingjiang Formation, Eastern Sichuan Basin. *J. Pet. Sci. Eng.* **2022**, *221*, 111–165. [CrossRef]
24. Tian, J.F.; Yu, J.; Zhang, Q.Z. Formation of chlorite in pore lining and its effect on reservoir quality. *J. Jilin Univ.* **2014**, *44*, 742–748. (In Chinese)
25. Xu, Y.M.; Yuan, B.L.; Zhang, H.; Ye, Q.; Huan, J.L. Reservoir physical characteristics and influencing factors of the third member of Weizhou Formation in Weizhou 12-X oilfield, Beibu Gulf Basin. *J. Northeast. Pet. Univ.* **2020**, *44*, 46–56. (In Chinese)
26. Zhang, S.W.; Yuan, J.; Sui, F.G.; Chen, X. Multiple diagenetic environments and evolution model in deep formation of the 4th Member, Shahejie Formation in the northern Dongying sag. *Chin. J. Geol.* **2008**, *43*, 576–587. (In Chinese)
27. Cao, Y.C.; Chen, L.; Wang, Y.Z. Diagenetic evolution of Es3 reservoir and its influence on property in the northern Minfeng sub-sag of Dongying sag. *J. China Univ. Pet. Ed. Nat. Sci.* **2011**, *35*, 6–13. (In Chinese)
28. Chen, H.H.; Li, C.Q.; Ping, H.W. *Reservoir Diagenesis and Quality Predication*; University of Geosciences of Press Co., Ltd.: Wuhan, China, 2012.
29. Beaufort, D.; Rigault, C.; Billon, S.; Billault, V.; Inoue, A. Chlorite and chloritization processes through mixed-layer mineral series in lowtemperature geological systems—A review. *Clay Miner.* **2015**, *50*, 497–523. [CrossRef]
30. Billault, V.; Beaufort, D.; Baronnet, A. A nanopetrographic and textural study of grain coats chlotites in sandstone reservoirs. *Clay Miner.* **2003**, *38*, 315–328. [CrossRef]

31. Huang, S.J.; Xie, W.; Zhang, M.; Wu, W.H.; Shen, L.C. Formation mechanism of authigenic chlorite and relation to preservation of porosity in nonmarine Triassic reservoir sandstones. *J. Chengdu Univ. Technol. Sci. Technol. Ed.* **2004**, *31*, 273–281. (In Chinese)
32. Tian, J.F.; Chen, Z.L.; Fan, Y.F.; Li, P.P.; Song, L.J. Occurrence mechanism and distribution of authigenic chlorite in sandstone. *Bull. Mineral. Petrol. Geochem.* **2008**, *27*, 200–207. (In Chinese)
33. Tian, J.F.; Chen, Z.L.; Yang, Y.Y. The protection mechanism of authigenic chlorite to sandstone reservoir pores. *Geol. Sci. Technol. Inf.* **2008**, *27*, 49–54. (In Chinese)
34. Chen, B.Z.; Li, R.X.; Liang, J.W. Study on the effect of authigenic chlorite on reservoir physical properties—The yanchang formation in the southwest margin of ordos basin is taken as an example. *Bull. Mineral. Petrol. Geochem.* **2014**, *33*, 390–394. (In Chinese)
35. Zhou, X.F.; Jiao, S.J.; Yu, J.M. Occurrences and origin of chlorite films in the Yanchang Formation sandstones, Ordos Basin. *Bull. Mineral. Petrol. Geochem.* **2017**, *36*, 834–842. (In Chinese)
36. Yan, Q.; Lei, H.Y.; Xian, B.Z. Influence of source rock properties on the development of authigenic chlorite in conglomerate reservoirs and its significance for oil and gas reservoirs: A case study from the Lower Urhe Formation in the Mahu Depression, Junggar Basin. *Acta Sedimentol. Sin.* **2020**, *38*, 367–378. (In Chinese)
37. Wu, J.Y.; Lv, Z.X.; Qing, Y.H.; Yang, J.J.; Jin, T. Genesis of Authigenic Chlorite in Tight Oil Reservoir and Its Effect on Physical Properties—A Case Study of Shaximiao Formation in Northeast Sichuan. *Lithol. Reserv.* **2020**, *32*, 76–85. (In Chinese)
38. Zheng, Z.Y.; Zuo, Y.H.; Wen, H.G.; Li, D.M.; Luo, Y.; Zhang, J.Z.; Yang, M.Y.; Zeng, J.C. Natural gas characteristics and gas-source comparisons of the lower Triassic Feixianguan formation, Eastern Sichuan basin. *Pet. Sci.* **2023**, *20*, 1458–1470. [CrossRef]
39. Jeffry, D.G. Origin and growth mechanism of authigenic chlorite in sandstones of the lower Vicksburg formation. South Texas. *J. Sediment. Res.* **2001**, *71*, 27–36.
40. Chen, G.S.; Meng, Y.L.; Huan, J.L.; Xiao, L.H.; Feng, D. Research progress on the origin of anomalously high porosity and permeability zone in clastics reservoirs in petroliferous basin. *Adv. Earth Sci.* **2021**, *36*, 922–936. (In Chinese)
41. Wu, Q.; Liu, Q.; Liu, S.; Wang, S.; Yu, J.; Ayers, W.B.; Zhu, Q. Estimating Reservoir Properties from 3D Seismic Attributes Using Simultaneous Prestack Inversion: A Case Study of Lufeng Oil Field, South China Sea. *SPE J.* **2022**, *27*, 292–306. [CrossRef]
42. Cao, Z.; Liu, G.D.; Meng, W.; Peng, W.; Cheng, Y.Y. Origin of different chlorite occurrences and their effects on tight clastic reservoir porosity. *J. Pet. Sci. Eng.* **2018**, *160*, 384–392. [CrossRef]
43. Worden, R.H.; Bukar, M.; Shell, P. The effect of oil emplacement on quartz cementation in a deeply buried sandstone reservoir. *AAPG* **2018**, *102*, 49–75. [CrossRef]
44. Guo, F.F.; Guo, X.W.; Sun, J.F. Source rock thermal and maturity history modeling in C sag of the weixinan depression, Bibuwan, Basin. *Mar. Geol. Quat. Geol.* **2010**, *30*, 87–93. (In Chinese)
45. Ying, F.X.; Luo, P.; He, D.B. *Diagenesis and Numerical Simulation of Clastic Reservoirs in Petroliferous Basins of China*; Petroleum Industry Press: Beijing, China, 2004; pp. 61–76.
46. Moard, S.; Aldahan, S.S. Diagenetic chloritization of feldspars in sandstones. *Sediment. Geol.* **1987**, *51*, 155–164. [CrossRef]
47. Ruiz Cruz, M.D.; Reyes, E. Kaolinite and dickite formation during shale diagenesis: Isotopic data. *Appl. Geochem.* **1998**, *13*, 95104. [CrossRef]
48. Hancock, N.J.; Taylor, A.M. Clay mineral diagenesis and oil migration in the Middle Jurassic Brent sand formation. *J. Geol. Soc. Lond.* **1978**, *135*, 69–72. [CrossRef]
49. Sommer, F. Diagenesis of Jurassic sandstones in the Viking Graben. *J. Geol. Soc. Lond.* **1978**, *135*, 63–67. [CrossRef]
50. Kantorowicz, J.D. The nature, origin and distribution of authigenic clay minerals from middle Jurassic Ravenscar and Brent group sandstones. *Clay Miner.* **1984**, *19*, 359375. [CrossRef]
51. Bath, A.H.; Milodowski, A.E.; Spiro, A.E. Diagenesis of carbonate cements in Permo-Triassis sandstones in the Wessex and East YorkshireLincolnshire basins, UK: A stable isotope study. In *Diagenesis of Sedimentary Sequences*; Marshall, J.D., Ed.; Special Publication 36; Geological Society: London, UK, 1987; p. 173190.
52. Lee, M.; Aronson, J.L.; Savin, S.M. Timing and conditions of Permian Rotliegende sandstone diagenesis, southern North Sea: K/Ar and oxygen isotopic data. *Am. Assoc. Pet. Geol. Bull.* **1989**, *73*, 195215.
53. Bjørlykke, K.; Aagaard, P. Clay minerals in North Sea sandstones. In *Origin, Diagenesis, and Petrophysics of Clay Minerals in Sandstones*; Houseknecht, D.W., Pittman, E.D., Eds.; SEPM Spec. Publ. 47; SEPM: Tulsa, OK, USA, 1992; p. 6580.
54. Haszeldine, S.; Brint, J.F.; Fallick, A.E.; Hamilton, P.J.; Brown, S. K-Ar dating of illites in Brent Group reservoirs. In *Geology of the Brent Group*; Morton, A.C., Haszeldine, R.S., Giles, M.R., Brown, S., Eds.; Special Publication 61; Geological Society: London, UK, 1992; p. 377400.
55. McAulay, G.E.; Burley, S.D.; Fallick, A.E.; Kuznir, N.J. Palaeohydrodynamic fluid flow regimes during diagenesis of the Brent group in the HuttonNW Hutton reservoirs: Constraints from oxygen isotope studies of authigenic kaolin and reverse flexural modelling. *Clay Miner.* **1994**, *29*, 609626. [CrossRef]
56. Purvis, K. Diagenesis of Lower Jurassic sandstones, Block 211/13 (Penguin area), UK northern North Sea. *Mar. Pet. Geol.* **1995**, *12*, 219228. [CrossRef]
57. Hancock, N.J. Possible causes of Rotliegend sandstone diagenesis in northern West Germany. *J. Geol. Soc.* **1978**, *135*, 35–40. [CrossRef]
58. Xu, T.T.; Wang, X.X.; Zhang, Y.Y. *Clay Minerals in Petroliferous Basin, China*; Petroleum Industry Press: Beijing, China, 2003; pp. 37–69.

59. Meng, F.J.; Xiao, L.H.; Xie, Y.H. Abnormal Transformation of the clay minerals in Yinggehai Basin and Its Significances. *Acta Sedimentol. Sin.* **2012**, *30*, 469–476. (In Chinese)
60. Stoessell, R.K. Kaolinite formation in clastic reservoirs: Carbon dixoid factor. *AAPG* **1981**, *65*, 998–999.
61. Dowey, P.J.; Hodgson, D.M.; Worden, R.H. Pre-requisites, processes, and prediction of chlorite grain coatss in petroleum reservoirs: A review of subsurface examples. *Mar. Pet. Geol.* **2012**, *32*, 63–75. [CrossRef]
62. Wu, S.J.; You, L.; Zhao, Z.J. Reservoir characteristics and favorable reservoir distribution of member three of Liushagang Formation of Xieyang Slope in Weixinan Sag. *J. Northeast Pet. Univ.* **2017**, *41*, 24–31. (In Chinese)
63. Sun, Z.L.; Huang, S.J.; Zhang, Y.X.; Wang, Q.D.; Bao, S.X.; Sun, Z.X. Origin and diagenesis of authigenic chlorite within the sandstone reservoirs of Xujiahe Formation, Sichuan Basin, China. *Acta Sedimentol. Sin.* **2008**, *26*, 459–468. (In Chinese)
64. Bjørkum, P.A.; Gjelsvik, N. An isochemical model for formation of authigenic kaolinite, K-feldspar, and illite in sediments. *J. Sediment. Petrol.* **1988**, *58*, 506–511.
65. Hower, J. Shale diagenesis. In *Short Course in Clays and Resource Geologist*; Mineralogical Association of Canada: Quebec, QC, Canada, 1981; pp. 60–77.
66. Xiao, Y.; Wang, R.C.; Lu, X.C.; Gao, J.F.; Xu, S.J. Experimental study on the low-temperature dissolution of microperthite in alkaline solution. *Acta Miner. Sin.* **2003**, *23*, 333–340. (In Chinese)
67. Hellmann, R. The albite-water system: Part I. The kinetics of dissolution as a function of pH at 100, 200, and 300 °C. *Geochim. Cosmochim Acta.* **1994**, *58*, 595–611. [CrossRef]
68. McKinley, J.M.; Worden, R.H.; Ruffell, A.H. Smectite in sandstones: A review of the controls on occurrence and behaviour during diagenesis. In *Clay Mineral Cements in Sandstones*; Worden, R.H., Morad, S., Eds.; Special Publications; International Association of Sedimentologists: Ghent, Belgium, 2003; Volume 34, pp. 109–128.
69. Gier, S.; Worden, R.H.; Krois, P. Comparing clay mineral diagenesis in interbedded sandstones and mudstones, Vienna Basin, Austria. *Geol. Soc. Spec. Publ.* **2015**, *435*, 389–403. [CrossRef]